

## Voltammetric Determination of Bisphenol A in the Presence of Uric Acid Using a Zn/Al-LDH-QM Modified MWCNT Paste Electrode

Nurashikin Abd Azis<sup>1</sup>, Ilyas Md Isa<sup>1,2,\*</sup>, Norhayati Hashim<sup>1,2</sup>, Mohamad Syahrizal Ahmad<sup>1,2</sup>, Siti Nur Akmar Mohd Yazid<sup>1</sup>, Mohamad Idris Saidin<sup>1</sup>, Suyanta M. Si<sup>3</sup>, Rahadian Zainul<sup>4</sup>, Alizar Ulianas<sup>4</sup>, Siriboon Mukdasai<sup>5</sup>

<sup>1</sup> Department of Chemistry, Faculty of Science and Mathematics, Universiti Pendidikan Sultan Idris, 35900 Tanjong Malim, Perak, Malaysia

<sup>2</sup> Nanotechnology Research Centre, Faculty of Science and Mathematics, Universiti Pendidikan Sultan Idris, 35900 Tanjong Malim, Perak, Malaysia

<sup>3</sup> Department of Chemistry Education, Faculty of Mathematics and Natural Science, Yogyakarta State University, Indonesia

<sup>4</sup> Department of Chemistry, Faculty of Mathematics and Natural Science, Universitas Negeri Padang, West Sumatera 25171, Indonesia

<sup>5</sup> Department of Chemistry, Faculty of Science, Khon Kaen University, Khon Kaen 40002, Thailand

\*E-mail: [illyas@fsmt.upsi.edu.my](mailto:illyas@fsmt.upsi.edu.my)

Received: 5 July 2019 / Accepted: 20 August 2019 / Published: 7 October 2019

---

A multiwalled carbon nanotube paste electrode (MWCNTPE) modified with zinc aluminium layered double hydroxide-quinmerac (Zn/Al-LDH-QM) was fabricated for simultaneous determination of uric acid and bisphenol A. This modified electrode was characterized by scanning electron microscope (SEM), transmission electron microscope (TEM), and electrochemical methods. Several experimental conditions such as percent of modifier, pH of the solution, and square wave voltammetry parameters were optimized. The effective surface area of the electrode were determined by chronocoulometry. There was several linear range where the sensor performs well which are within the concentration 0.3 – 30.0  $\mu\text{M}$  and 50.0 – 100.0  $\mu\text{M}$  for uric acid, and 0.3 – 50.0  $\mu\text{M}$  and 10.0 – 100.0  $\mu\text{M}$  for bisphenol A. The detection limit for both organics were 0.065  $\mu\text{M}$  and 0.049  $\mu\text{M}$ , respectively. The modified MWCNTPE was also tested for the determination of uric acid and bisphenol A in real samples and achieved high recoveries percentage from 98.0% to 108.3 %.

---

**Keywords:** Layered double hydroxide, Modified electrode, Bisphenol A, Uric acid

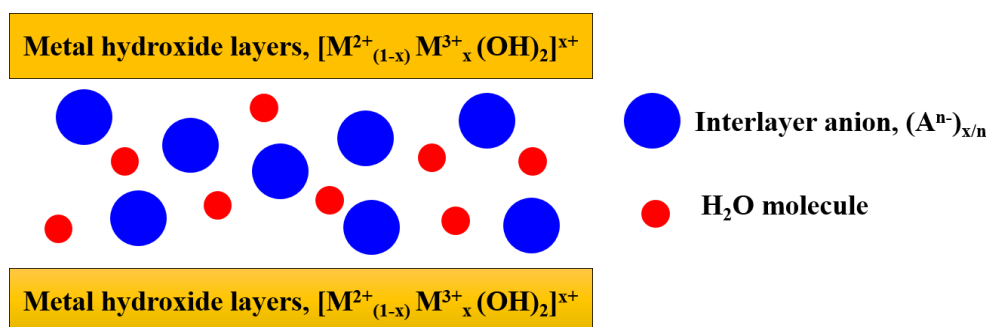
### 1. INTRODUCTION

Bisphenol A (BPA) is an important monomer, used in the production of plastics and exists in many consumer products such as water bottles, feeding bottles, as well as reusable food and drink

containers. BPA can leaches from these materials and enters into foodstuff [1,2]. It cause harm to human as this chemical belongs to a group of endocrine-disrupting compound, and its toxicity is widely reported in literature [3]. It has been shown that the urine is a suitable marker for monitoring of BPA because almost 100% orally administered BPA is excreted via urine [4,5]. In addition, studies also have shown that BPA is frequently found in waste water, river water, and sea water [6,7]. On the other hand, uric acid (UA) is a final product of purine metabolism, and the oxidation of electroactive UA in an aqueous solution can yield to allantoin as a major product, which is freely eliminated by urine [8]. Abnormal levels of UA are associated with gout disease, whereas the formation of UA crystal which eventually grow into stones causing harm to human organ such as kidney [9,10].

The commonly use methods for BPA and UA determination include colorimetric [11] and fluorometric [12], spectrophotometric [13] and spectrofluorimetric [14], solid phase extraction [15], and high performance-liquid chromatography [16]. However, these method are neither economical nor user-friendly for routine analysis. Therefore, it is desirable to develop analytical methods that are simple, low-cost, user friendly and high sensitivity as well as selectivity. Fortunately, these advantages owned by electrochemical sensor. The utilization of carbon paste electrode (CPE) fabricated with carbon nanotube (CNT) has shown great performance in electrochemical sensor [17,18]. Apart from that, layered double hydroxides (LDHs) (**Scheme 1**) have gained much attention in CPE fabrication due to their remarkable capability of anion exchange. The raising attention in LDH also comes from their versatile properties in terms of surface area, low toxicity and chemical inertness [19]. Related work in determination of various analytes by using LDH have been reported [20-22].

However, there is still no report on the use of LDH in simultaneous determination of BPA and UA. Therefore, in this work, a multiwalled carbon nanotube paste electrode (MWCNTPE) modified with zinc aluminium layered double hydroxide-quinmerac (Zn/Al-LDH-QM) has been fabricated for simultaneous determination of BPA and UA.



**Scheme 1.** Illustration of layered double hydroxide.

## 2. EXPERIMENTAL

### 2.1. Chemicals

The MWCNTs were purchased from Timesnano (China). BPA and UA were purchased from Sigma-Aldrich Co. (USA).  $1 \times 10^{-2}$  M UA and BPA stock solution were prepared with ethanol and

sodium hydroxide, respectively and kept in refrigerator at 4°C. Potassium phosphate buffer solution (PBS) was prepared by mixing the stock solution of 0.1 M  $K_2HPO_4$  and 0.1 M  $KH_2PO_4$ .

## 2.2. Apparatus

Electrochemical experiments were conducted using a Potentiostat Ref 3000 and Potentiostat Series-G750. An electrochemical workstation consisting of modified MWCNT paste electrode as a working electrode, Ag/AgCl electrode as a reference electrode and platinum wire as a counter electrode. The surface morphology of Zn/Al-LDH-CP/MWCNT was observed using field emission scanning electron microscopy (FESEM), model SU8020 UHR (Hitachi, Japan) and transmission electron microscope (TEM), model JEOL-2000EX (Japan). The pH measurements were carried out on a Thermo Scientific Orion 2-Star Benchtop pH Meter.

## 2.3. Synthesis of zinc/aluminium-layered double hydroxide-quinmerac nanocomposites (Zn/Al-LDH-QM)

Zn/Al-LDH were synthesized by a conventional co-precipitation method, where  $Zn(NO_3)_2$  and  $Al(NO_3)_3$  were used as a precursors [23]. Both precursors were dissolved in 250 mL of deionized water and 50 mL of 0.1 M quinmerac (QM) solution was added. The mixture was stirred until the homogenized solution was produced. A few drops of sodium hydroxide were used to adjust the pH of the solution until reach pH 7.5. The mixture was left in oil bath shaker at 70°C for 24 hours. Then the slurry was centrifuged, washed and dried in oven at 60°C. The dried precipitate of Zn/Al-LDH-QM was finely ground and kept in a bottle at room temperature.

## 2.4. Electrode preparation

Zn/Al-LDH-QM (0%, 5%, 10%, 15%) and MWCNTs (100%, 95%, 90%, 85%) were mixed using a mortar and pestle with a few drops of paraffin oil. The homogenized paste was then tightly pressed into a Teflon tube, with one of the tube end was connected to a copper wire to produce established electrical contact. The surface was smoothened on a soft paper before each measurements.

# 3. RESULTS AND DISCUSSION

## 3.1. Characterization of Zn/Al-LDH-QM/MWCNTs

The Zn/Al-LDH-QM/MWCNTs materials were characterized by SEM and TEM, with the results shown in **Fig. 1A** and **Fig. 1B**, respectively. The SEM image shows irregular and petals-like structure of Zn/Al-LDH-QM attached within a bundle of MWCNTs. The morphology of Zn/Al-LDH intercalated with QM was agreed with the one which discovered in the previous study [23]. The flake features of Zn/Al-LDH-QM were also remained under TEM view.

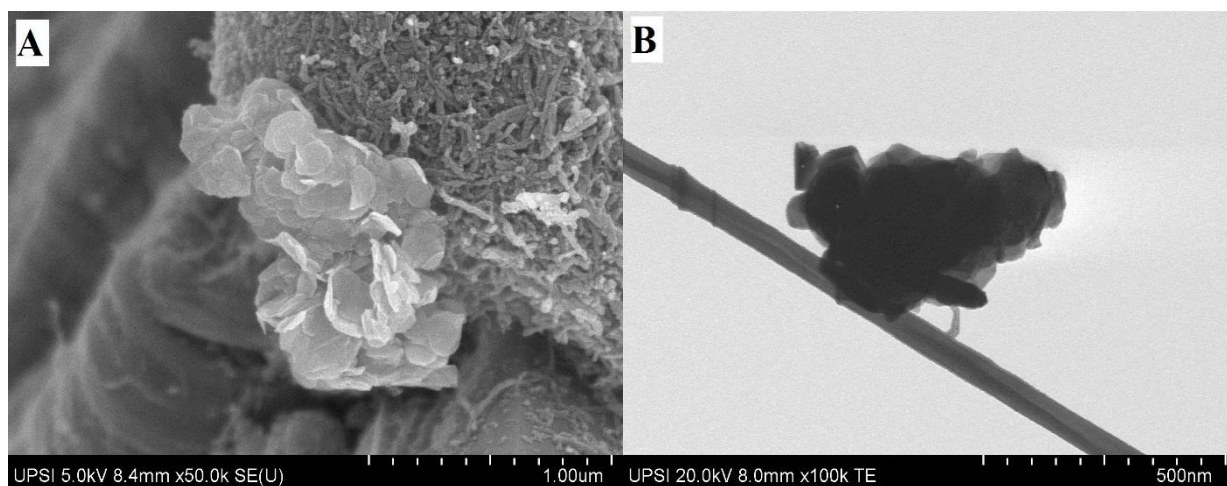


**Figure 1.** (A) SEM image of Zn/Al-LDH-QM and (B) TEM image of Zn/Al-LDH-QM/MWCNT mixture.

### 3.2. Characterization of sensor fabrication

Cyclic voltammetry measurement was performed for unmodified and modified multiwalled carbon nanotube paste electrodes (MWCNTPE) in  $4.0 \times 10^{-3}$  M  $K_3[Fe(CN)_6]$ . This redox couple has been a recommended choice as a standard to demonstrate cyclic voltammetry because they exhibit nearly a reversible electrode reaction [24]. **Fig. 2** shows the electrochemical response of  $K_3[Fe(CN)_6]$  at both electrodes. Due to the bare properties, the unmodified MWCNTPE exhibited a low current signal; anodic peak current ( $I_{pa}$ ) and cathodic peak current ( $I_{pc}$ ) were  $6.636 \mu A$  and  $3.865 \mu A$ , respectively. However, the voltammetric response is apparently improved at modified MWCNTPE with redox peak currents increased to  $I_{pa} = 11.44 \mu A$  and  $I_{pc} = 8.826 \mu A$ . Additionally, the peak-to-peak separation ( $\Delta E_p$ ) also declined from  $591.8$  mV to  $367.8$  mV, which could be due to the higher electron transfer rate at the surface of modified electrode compared to unmodified electrode, although both electrodes experienced the reversible reaction of  $K_3[Fe(CN)_6]$ . These results suggested that the implementation of Zn/Al-LDH-QM to the modification of MWCNTPE contributed in an excellent electrochemical response of the electrode.

The CV results were supported by the findings obtained from electrochemical impedance spectroscopy (EIS) studies. In general, the semicircle portion of the EIS represents the electron transfer-limited process, and the linear portion corresponds to the diffusion-limited process. The diameter of semicircle corresponds to the charge transfer resistance ( $R_{ct}$ ) at the electrode surface. **Fig. 3** illustrated Nyquist plots of unmodified and modified MWCNTPE. The unmodified MWCNTPE exhibits a large semicircle, compared to the modified MWCNTPE, which the  $R_{ct}$  value of the former was almost two times larger than the latter. This ease of transfer of electrons to and from the electrode surface minimizes the charge transfer resistance. In addition, the electron transfer apparent rate constant ( $k_{app}$ ) value for both electrodes were calculated from below equation.

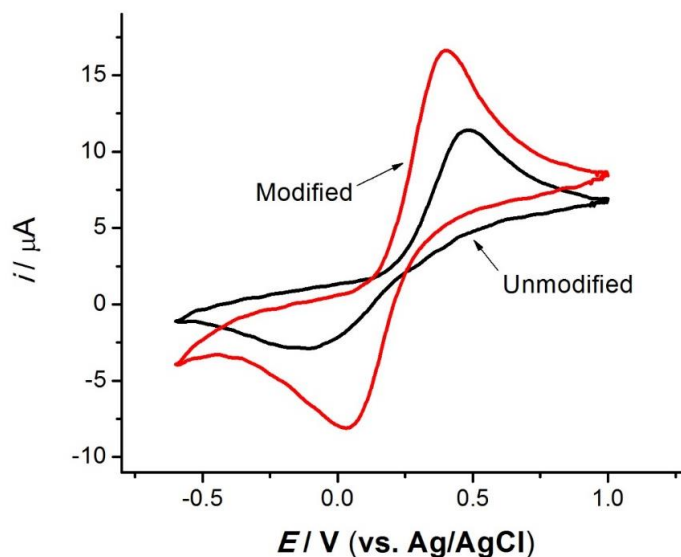


**Figure 2.** Cyclic voltammograms of unmodified and modified MWCNT paste electrodes in  $4.0 \times 10^{-3}$  M  $K_3[Fe(CN)_6]$  containing 0.1 M KCl. Scan rate  $100 \text{ mVs}^{-1}$ .

$$k_{app} = \frac{RT}{F^2 R_{ct} AC}$$

Where  $R$ ,  $T$  and  $F$  have their usual meanings,  $A$  is the estimated surface area of electrode, and  $C$  is the concentration of the  $K_3[Fe(CN)_6]$  solution. Due to the relationship between charge transfer resistance and the electron transfer rate across the interface [25], the  $k_{app}$  values were calculated for unmodified and modified MWCNTPEs to be  $8.95 \times 10^{-5} \text{ cm s}^{-1}$  and  $1.48 \times 10^{-4} \text{ cm s}^{-1}$ , respectively. The modified MWCNT showed high  $k_{app}$  and low  $R_{ct}$  values which indicated a faster electron transfer process. This process has been accelerated by the presence of Zn/Al-LDH-QM.

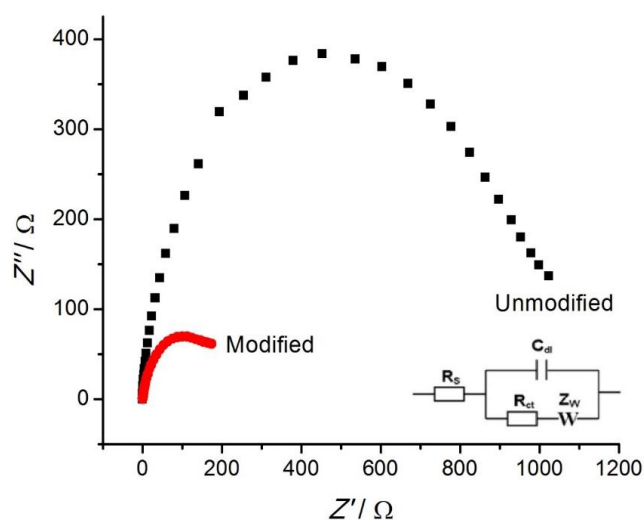


**Figure 3.** Nyquist plot of unmodified and modified MWCNT paste electrodes in  $4.0 \times 10^{-3}$  M  $K_3[Fe(CN)_6]$  containing 0.1 M KCl. Inset: Randle's equivalent electrical circuit system.

### 3.3. Optimization of the experimental conditions

#### 3.3.1. Percentage of modifiers

The influence of the percentage of Zn/Al-LDH-QM used as modifier in carbon paste composition towards the electrochemical response of  $1.0 \times 10^{-4}$  M of BPA and UA solution were investigated using square wave voltammetry. **Fig. 4** shows the current response towards the modification of MWCNTPE with different percentage of Zn/Al-LDH-QM. The modification of MWCNTPE with 5:95 (%) ratio of Zn/Al-LDH-QM to MWCNTs exhibited the highest current peak due to increase in the conductive area on the electrode surface [26]. Further increased in the amount of modifier cause the current response to decreased possibly due to the alteration of the physical and physiochemical properties of the electrode surface [27]. Therefore, the modified MWCNTPE with 5% of Zn/Al-LDH-QM was implemented for subsequent experiments.

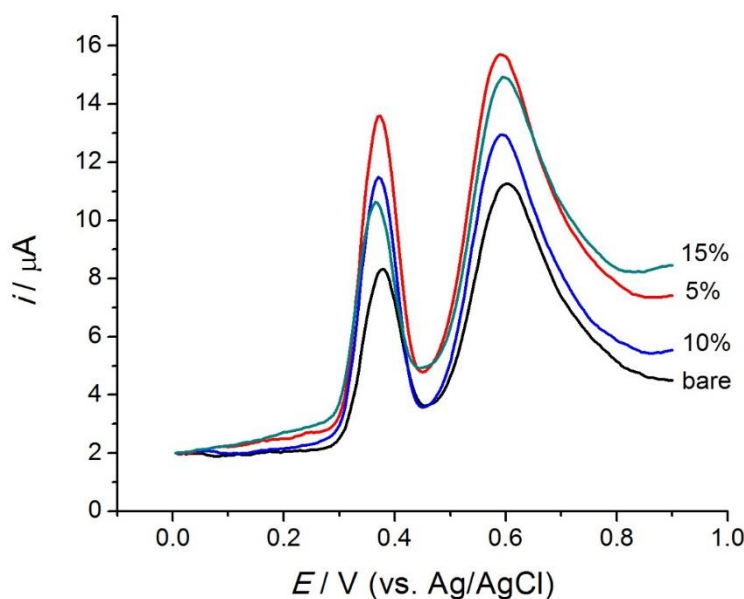


**Figure 4.** Graph of different composition ratios (%w/w) of Zn/Al-LDH-QM at modified MWCNT paste electrode.

#### 3.3.2. pH effect

The pH ranges of 5.4 to 7.4 were studied for the electrochemical response of  $1.0 \times 10^{-4}$  M of UA and BPA solution. As can be seen in **Fig. 5**, the highest current peak exhibited by pH 6.0 for both UA and BPA. While going towards the basic condition of the solution, the decreasing of current peak was observed. The reduce in the current response at pH lower than 6.0 might be due to the competition between the hydrogen ions and the cation of the analytes to be deposited on the electrode surface, while at pH higher than 6.0, the current response decrease possibly due to the formation of hydroxyl compound [28]. Thus, a pH 6.0 was chosen for the subsequent analytical experiments.

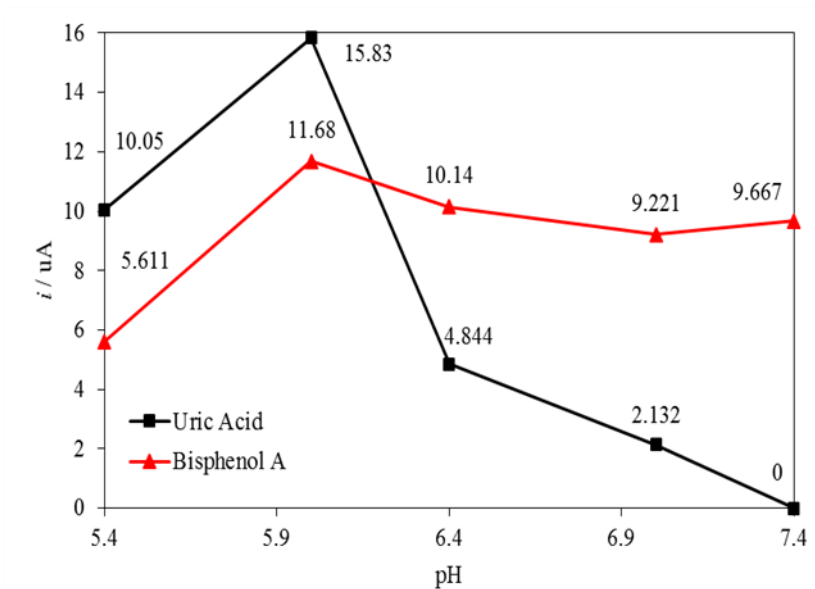


**Figure 5.** Effects of pH value on the current response of  $1 \times 10^{-4}$  M UA and BPA mixture.

### 3.3.3. Square wave voltammetry parameters

In square wave voltammetry (SWV) measurement, optimization of several parameters are taken into account as they may affect the electrode performance [29]. As shown in **Fig. 6A**, the effect of frequency was evaluated by increasing the frequency from 90 to 190 Hz. The current peak was increased up to 170 Hz and started to decrease at the frequency over 170 Hz. The measurements were continued by varied the step size from 1 to 5 mV, and resulted the highest current peak at step size 4 mV (**Fig. 6B**). The pulse size was measured from 10 to 60 mV. As shown in **Fig. 6C**, the highest current peak has been exhibited by pulse size of 50 mV. Thus, the optimum parameters used for subsequent experiments were at frequency 170 Hz, step size 4 mV and pulse size 50 mV.

### 3.3.4. Scan rate effect

**Fig. 7A** and **Fig. 7B** shows cyclic voltammograms of  $1.0 \times 10^{-4}$  M UA and BPA with different scan rates. Meanwhile, the inset graphs were plot of peak current versus scan rate ( $v$ ), which was observed to be directly proportional to one another. The equation can be expressed as  $I_{pa} (\mu A) = 0.021v (mVs^{-1}) + 8.109$  ( $R^2 = 0.9938$ ) for UA, and  $I_{pa} (\mu A) = 0.021v (mVs^{-1}) - 1.243$  ( $R^2 = 0.9956$ ) for BPA. In this case, the deviations from linearity in plots of peak current versus square root of the scan rate (Randles-Sevcik equation) suggested that electron transfer may be occurring via a surface adsorption-controlled process. No peak-to-peak separation was observed also acts as an indication of a surface adsorption-controlled process of UA and BPA at the surface of the Zn/Al-LDH-QM/ MWCNTPE [24].



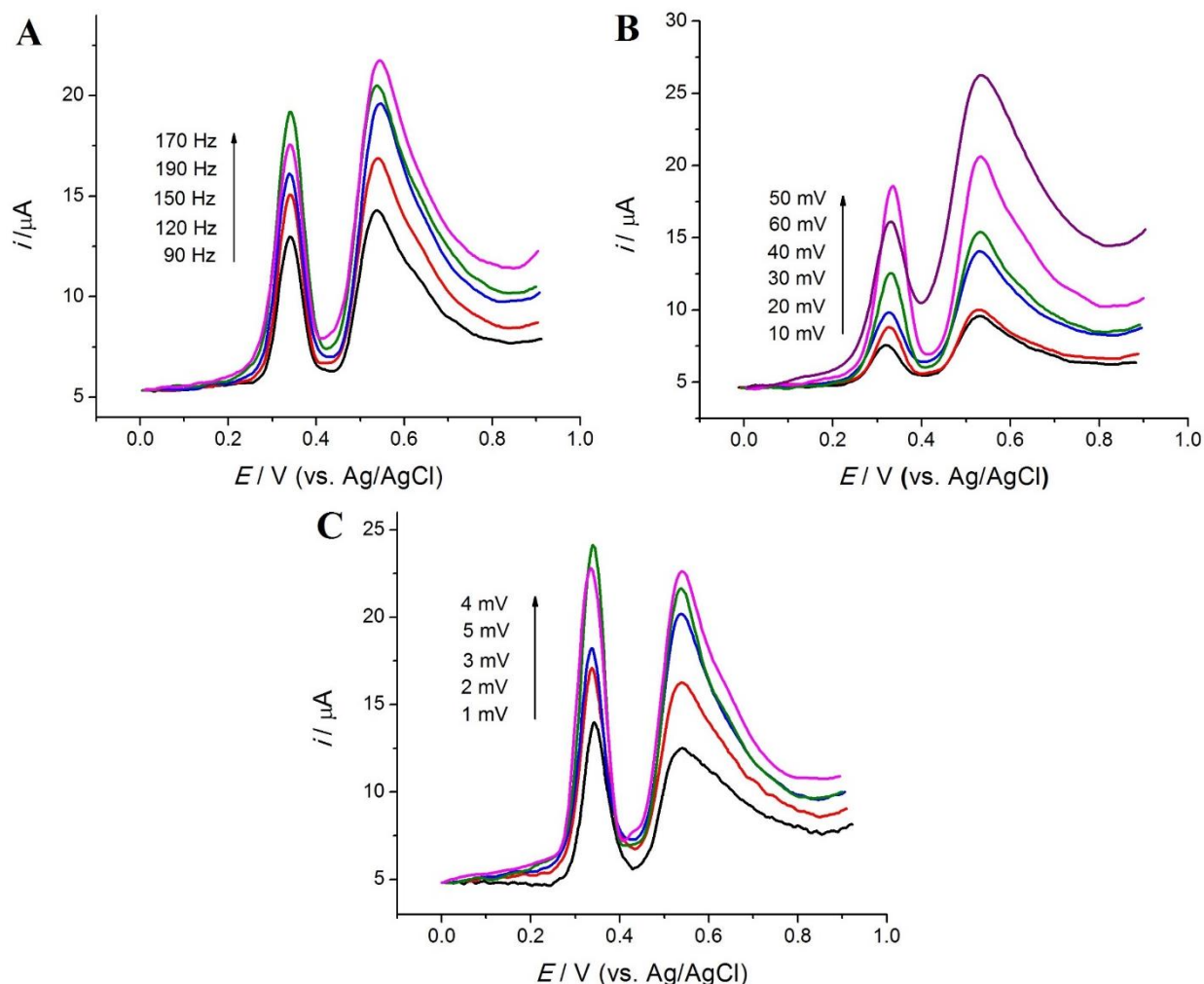


**Figure 6.** Effects of the SWV parameters (A) frequency, (B) pulse size, and (C) step size on current response. Solution:  $1 \times 10^{-4}$  M UA and BPA mixture.

### 3.3.5. Chronocoulometry studies

Chronocoulometry studies were performed to determine the effective surface area,  $A$ , of both unmodified and modified MWCNTPEs.  $4.0 \times 10^{-3}$  M  $K_3[Fe(CN)_6]$  solution was used as a model complex. The  $A$  was calculated based on Anson equation:

$$Q(t) = \frac{2nFAcD^{\frac{1}{2}}t^{\frac{1}{2}}}{\pi^{\frac{1}{2}}} + Q_{dl} + Q_{ads}$$

Where  $Q(t)$  is charge,  $n$  in number of electron transfer,  $F$  is Faraday constant (96485 Coulombs/mole),  $c$  is concentration of substrate, and  $D$  is diffusion coefficient of  $K_3[Fe(CN)_6]$ . According to the slopes of the plots of  $Q$  vs.  $t^{1/2}$  (**Fig. 8A**), the effective electrochemical surface area for unmodified MWCNTPE was calculated as  $0.016 \text{ cm}^2$ , and  $0.059 \text{ cm}^2$  for modified MWCNTPE. These indicated that the modification of MWCNT paste electrode with Zn/Al-LDH-QM increased the



electrode effective surface area. This phenomenon would increase the adsorption site, and further enhance the electrochemical performance of the sensor [30].

The chronocoulometry experiments were then carried out on the modified MWCNTPE in  $1.0 \times 10^{-4}$  M UA and BPA solution. A plot of charge ( $Q$ ) against the square root of time ( $t^{1/2}$ ) (Fig.8B) was obtained after background subtraction and exhibited a slightly linear relationship. Hence,  $D$  for UA and BPA were calculated to be  $1.09 \times 10^{-3}$  cm<sup>2</sup> s<sup>-1</sup> and  $1.90 \times 10^{-3}$  cm<sup>2</sup> s<sup>-1</sup>, respectively. Based on Cottrell equation,  $Q_{ads} = nFA\Gamma_s$ , the adsorption capacity,  $\Gamma_s$ , for UA and BPA can be obtained as  $1.72 \times 10^{-8}$  mol cm<sup>-2</sup> and  $1.95 \times 10^{-8}$  mol cm<sup>-2</sup>, respectively.

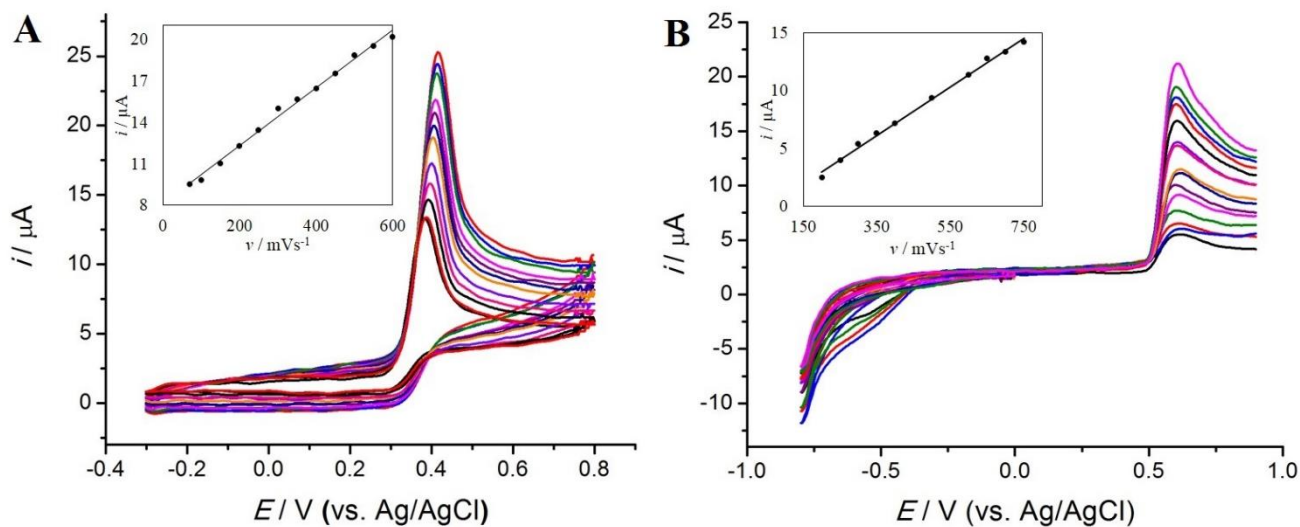


**Figure 7.** Cyclic voltammogram of Zn/Al-LDH-QM/MWCNT paste electrode with the different scan rates in  $1 \times 10^{-3}$  M of (A) UA and (B) BPA.

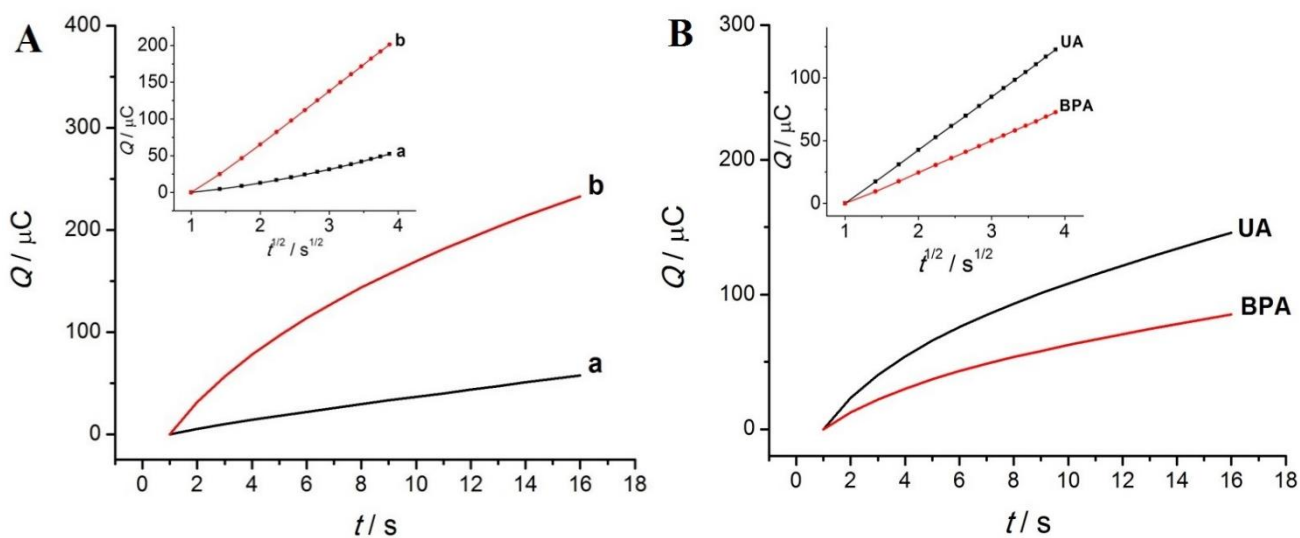


**Figure 8.** (A) Chronocoulograms of (a) MWCNT paste electrode, and (b) Zn/Al-LDH-QM/MWCNT paste electrode in  $4.0 \times 10^{-4}$  M  $K_3[Fe(CN)_6]$ , (B) Chronocoulograms of Zn/Al-LDH-QM/MWCNT paste electrode in  $1 \times 10^{-4}$  M (a) UA and (b) BPA solution.

### 3.3.6. Calibration plot

By using SWV, the modified MWCNTPE was applied for the successive determination of UA and BPA. Two working ranges were obtained for UA, i.e. from 0.3 – 30.0  $\mu\text{M}$  and 50.0 – 100.0  $\mu\text{M}$  (**Fig. 9A**). The linear regression equations of the first and second working range are  $y = -51.91x + 235.81$  ( $R^2 = 0.9875$ ) and  $y = -0.9289x + 6.207$  ( $R^2 = 0.9954$ ), respectively. Two working ranges were also obtained for BPA, i.e. from 0.3 – 50.0  $\mu\text{M}$  and 10.0 – 100.0  $\mu\text{M}$  (**Fig. 9B**). The linear regression equations of the first and second working range are  $y = -10.67x + 55.54$  ( $R^2 = 0.9969$ ) and  $y = -1.368x + 9.133$  ( $R^2 = 0.9956$ ), respectively. The detection limit of 0.065  $\mu\text{M}$  UA and 0.049  $\mu\text{M}$  BPA were obtained. The performance of the modified MWCNTPE in determination of UA and BPA was compared to those method reported earlier (**Table 1**). The proposed mechanism of analytes at the surface of the modified MWCNTPE also shown in **Scheme 2**.

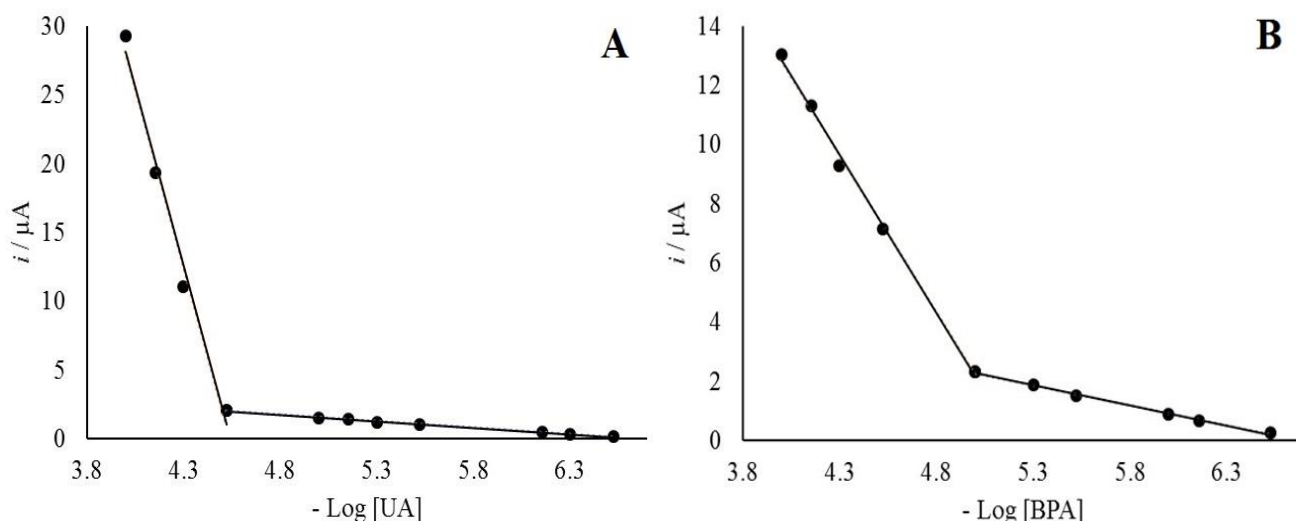


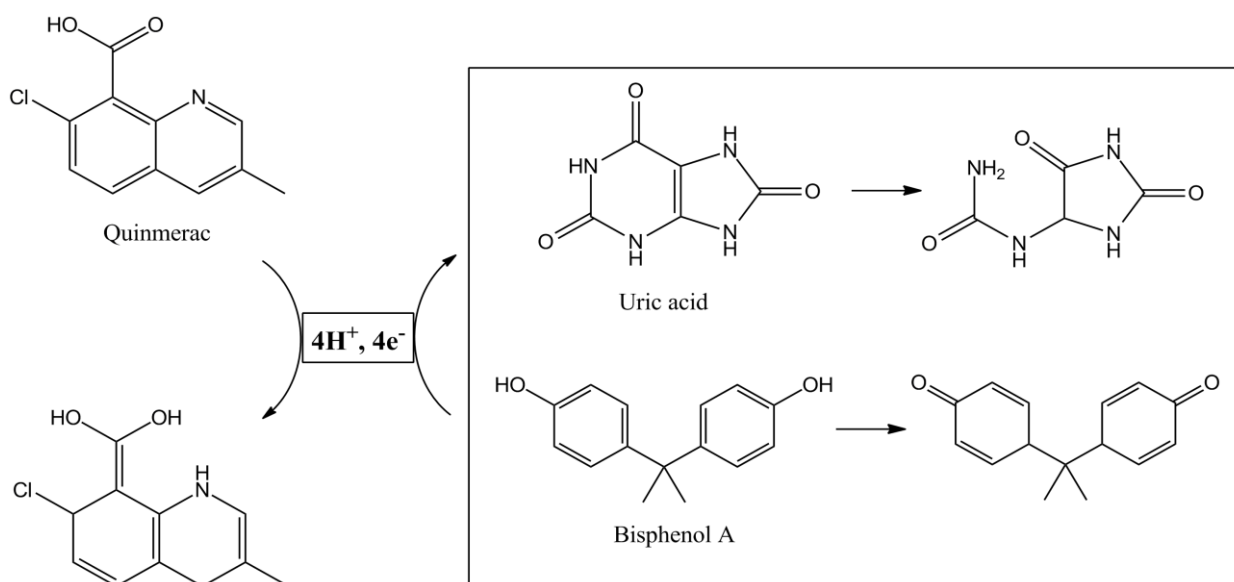
**Figure 9.** Calibration plot current peak versus  $-\text{Log}$  analytes concentration of various concentration of (A) UA and (B) BPA.

### 3.3.7. Repeatability

The repeatability of the sensor was taken into account in this study by carried out a series of repetitive measurements (**Fig. 10**). Relative standard deviation (RSD) of 2.98 % and 2.73 % were obtained for UA and BPA, respectively. These indicated that the modified electrode has a good repeatability.

**Table 1.** Comparison between the current work and some reported sensors for the individual and simultaneous determination of UA and BPA.

Determination	Analyte	Modifier/electrode	LWR <sup>a</sup> ( $\mu\text{M}$ )	DL <sup>b</sup>	Ref.
Individual	UA	Poly( $\beta$ -cyclodextrin)/CNT/ionic liquid/CPE	0.6 – 400.0	0.300	[[31]
		Mn(III) porphyrin-graphene/GCE	0.5 – 500.0	0.300	[[32]
		Au-cysteine-bentonite/GCE	1.0 – 200.0	0.930	[[33]
		Fe <sub>3</sub> O <sub>4</sub> @SiO <sub>2</sub> /GO/GCE	0.5 – 250.0	0.070	[[34]
	BPA	CdO NPs/ionic liquid/CPE	0.3 – 650.0	0.100	[[35]
		rGO/Cu <sub>2</sub> O nanocomposite/GCE	0.1 – 80.0	0.053	[[36]
		rGO-Ag/poly-L-lysine/GCE	1.0 – 80.0	0.540	[[37]
		Chitosan-graphene/GCE	5.0 – 200.0	0.340	[[38]
Simultaneous	UA	Zn-Al-LDH-QM/MWCNT/CPE	0.3 – 30.0, 50.0 – 100.0	0.065	This work
	BPA		0.3 – 50.0, 10.0 – 100.0	0.049	

<sup>a</sup> LWR – Linear working range.<sup>b</sup> DL – Detection limit.**Scheme 2.** Proposed reaction mechanism of UA and BPA at the surface of modified MWCNT paste electrode.

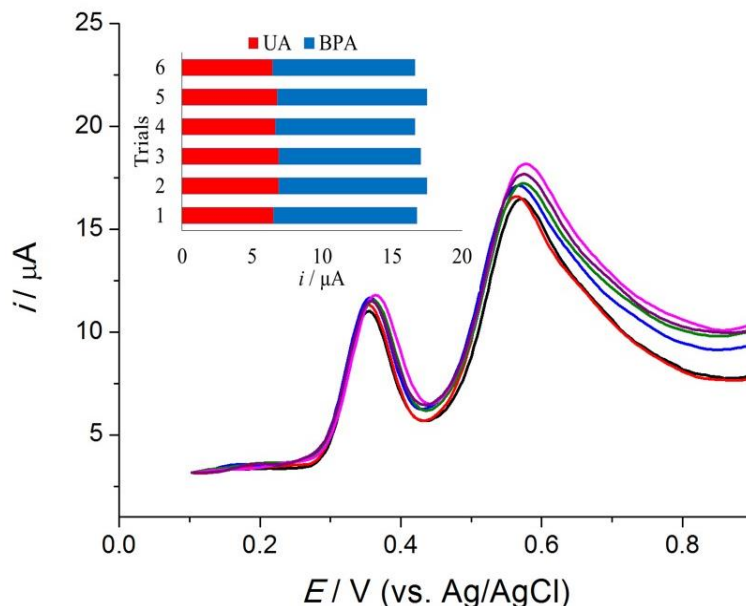


**Figure 10.** Repeatability of the modified MWCNT paste electrode.

3.3.8. Interferences studies

In order to evaluate the selectivity of the modified MWCNTPE, the influence of some potential interferences in  $1.0 \times 10^{-4}$  M UA and BPA solution was investigated. As shown in **Fig. 11**, the results indicated that most possible inorganic interferences, such as 10-fold and 50-fold concentration of ascorbic acid, glucose, sucrose, sodium salicylate, glutamic acid, phthalate, acetaminophen, captopril, dopamine, and hydroquinone did not interfere the electrochemical response of UA and BPA with the peak current changes less than  $\pm 10\%$ .

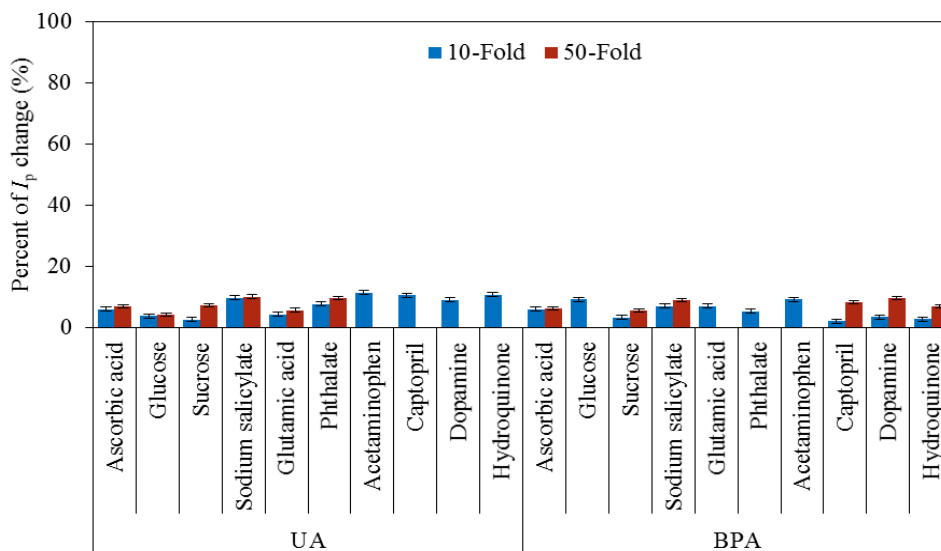


**Figure 11.** The influence of interferences in determination of UA and BPA at Zn/Al-LDH-QM/MWCNT paste electrode.

### 3.3.9 Real sample analysis

The feasibility of the modified MWCNTPE was tested with urine and water samples. The urine samples were collected from two healthy person and diluted 100 times with PBS buffer (pH 6), then analyzed without other pretreatment [39]. The lake water and sea water were collected from Tasik Embayu and Pantai Teluk Batik, respectively. One milliliter of each sample solution was mixed with 9 mL PBS buffer (pH 6) and then analyzed [40]. No BPA was detected in the water samples. Both urine and water samples were then analyzed by the standard addition method and the recoveries were calculated. The results are shown in **Table 2**. The high recovery (98.0 - 108.3 %) indicated that the modified MWCNTPE is appropriate for the analysis of real samples.

**Table 2.** Recoveries of UA and BPA in various samples.

Sample	Detected ( $\mu\text{M}$ )		Added ( $\mu\text{M}$ )		Found ( $\mu\text{M}$ )		Recovery (%)	
	UA	BPA	UA	BPA	UA	BPA	UA	BPA
Urine 1	22.3	N.D. <sup>a</sup>	4.0	12.0	27.3	11.9	103.9	99.7
Urine 2	22.1	N.D.	4.0	12.0	26.4	11.8	100.9	98.0
Lake water	N.D.	N.D.	10.0	10.0	9.9	10.6	99.5	105.5
Sea water	N.D.	N.D.	10.0	10.0	10.5	10.8	105.0	108.3

<sup>a</sup> ND – Not detected.

## 4. CONCLUSIONS

The role of Zn/Al-LDH-QM as a mediator in the simultaneous determination of UA and BPA was successfully demonstrated. The Zn/Al-LDH-QM/ MWCNTPE shows a good conductivity with high electron transfer rate through CV and EIS studies. The modified electrode also exhibits a large effective electrochemical surface area and high adsorption capacity. The developed sensor was free from interference of ascorbic acid, glucose, sucrose, sodium salicylate, glutamic acid, phthalate, acetaminophen, captopril, dopamine, and hydroquinone. At optimal condition, the electrode shows a wide linear range of UA and BPA concentration with a detection limit of 0.065  $\mu\text{M}$  and 0.049  $\mu\text{M}$ , respectively. The electrode also applicable for UA and BPA analysis in urine and water samples.

## ACKNOWLEDGEMENTS

The authors would like to thank Ministry of Education Malaysia and Universiti Pendidikan Sultan Idris for providing the respective financial support Grant nos.: FRGS 2017-0075-101-02 for this work.

## References

1. J.H. Kang, K. Kito and F. Kondo, *J. Food Prot.*, 66 (2003)1444.
2. C. Brede, P. Fjeldal, I. Skjevrak and H. Herikstad, *Food Addit. Contam.*, 20 (2003) 684.
3. L.N. Vandenberg, R. Hauser, M. Marcus, N. Olea and W.V. Welshons, *Reprod. Toxicol.*, 24

- (2007) 139.
4. J.W. Brock, Y. Yoshimura, J.R. Barr, V.L. Maggio, S.R. Graiser, H. Nakazawa and L.L. Needham, *J. Expo. Sci. Environ. Epidemiol.*, 11 (2001) 323.
  5. K.A. Thayer, D.R. Doerge, D. Hunt, S.H. Schurman, N.C. Twaddle, M.I. Churhwell, S. Garantziotis, G.E. Kissling, M.R. Easterling, J.R. Bucher and L.S. Birnbaum, *Environ. Int.*, 83 (2018) 107.
  6. Y.Q. Huang, C.K.C. Wong, J.S. Zheng, H. Bouwman, B. Wahlstrom, L. Neretin and M.H. Wong, *Environ. Int.*, 42 (2012) 91.
  7. A. Careghini, A.F. Mastorgio, S. Saponaro and E. Sezenna, *Environ. Sci. Pollut. Res.*, 22 (2015) 5711.
  8. B.A. Lario and J. M.Vicente, *Rheumatology*, 49 (2010) 2010-5.
  9. G. Nuki and P.A. Simkin, *Arthritis. Res. Ther.*, 8 (2006) 1.
  10. P.M. Ferraro and G.C. Curhan, *Am. J. Kidney. Dis.*, 70 (2017) 158.
  11. Y. Zhang, Y. Wang, W. Zhu, J. Wang, X. Yue, W. Liu, D. Zhang and J. Wang, *Microchim. Acta*, 184 (2017) 951.
  12. Y. Wang, Y. Yang, W. Liu, F. Ding, Q. Zhao, P. Zou, X. Wang and H. Rao, *Microchim Acta*, 185 (2018) 281.
  13. H.H. Hamzah, Z.M. Zain, N.L.W. Musa, Y.C. Lin and E. Trimbee, *J. Anal. Bioanal. Tech.*, S7 (2013).
  14. C.F. Nascimento and F.R.P. Rocha, *Microchem. J.*, 137 (2018) 429.
  15. S. Chen, J. Chen and X. Zhu, *Microchim. Acta*, 183 (2016) 1315.
  16. D. Li, X. Ma, R. Wang and Y. Yu, *Anal. Bioanal. Chem.*, 409 (2017) 1165.
  17. I. Švancara and K. Schachl, *Chem. Listy*, 93 (1999) 490
  18. A.J.S. Ahammad, J.J. Lee and M.A. Rahman, *Sensors*, (2009) 2289.
  19. D. Tonelli, E. Scavetta and M. Giorgetti, *Anal. Bioanal. Chem.*, 405 (2013) 603.
  20. I.M. Isa, S. Saruddin, N. Hashim, M. Ahmad and S.A. Ghani, *Int. J. Electrochem. Sci.*, 11 (2016) 4619.
  21. M.S. Ahmad, I.M. Isa, N. Hashim, S.M. Si and M.I. Saidin, *J. Solid State Electrochem.*, 22 (2018) 2691.
  22. M.S. Ahmad, I.M. Isa, N. Hashim, M.S. Rosmi and S. Mustafar, *Int. J. Electrochem. Sci.*, 13 (2018) 373
  23. N. Hashim, S.N.M. Sharif, I.M. Isa, M. Mamat, N.M. Ali, S.A. Bakar, M.Z. Hussein, , N.A. Bakar and W.R.W. Mahamod, *Res. J. Chem. Environ.*, 23 (2019) 36.
  24. N. Elgrishi, K.J. Rountree, B.D. McCarthy, E.S. Rountree, T.T. Eisenhart, J.L. Dempsey, *J. Chem. Educ.*, 95 (2018) 197.
  25. A. Sharma, J.K. Bhattarai, S.S. Nigudkar, S.G. Pistorio, A.V. Demchenko, K.J. Stine, *J Electroanal. Chem.*, 782 (2016) 174.
  26. H.R. Zare, Z. Sobhani, M. Mazloun-Ardakani, *Sensor Actuat. B-Chem.*, 126 (2007) 641.
  27. I. Švancara, K. Vytřas, J. Barek, J. Zima, *Crit. Rev. Anal. Chem.*, 31 (2001) 311.
  28. M.I. Saidin, I.M. Isa, M. Ahmad, N. Hashim, S.A. Ghani, *Sensor Actuat. B-Chem.*, 240 (2017) 848.
  29. J.G. Osteryoung and R.A. Osteryoung, *Anal. Chem.*, 57 (1985)101A.
  30. X. Dong, X. Qi, N. Liu, Y. Yang and Y. Piao, *Sensors*, 17 (2017) 836.
  31. Y. Li, X. Zhai, H. Wang, X. Liu, L. Guo, X. Ji, L. Wang, H. Qiu and X. Liu, *Microchim. Acta*, 182 (2015)1877.
  32. X.M. Guo, B. Guo, C. Li and Y.L. Wang, *J. Electroanal. Chem.*, 783 (2016) 8.
  33. D.K. Yadav, R. Gupta, V. Ganesan and P.K. Sonkar, *Microchim. Acta*, 184 (2017) 1951
  34. K. Movlaee, P. Norouzi, H. Beitollahi, M. Rezapour and B. Larijani, *Int. J. Electrochem. Sci.*, 12 (2017) 3241.
  35. V. Arabali, M. Ebrahimi, S. Gheibi, F. Khaleghi, M. Bijad, A. Rudbaraki, M. Abbasghorbani

- and M.R. Ganjali, *Food Anal. Methods*, 9 (2016) 1763.
36. R. Shi, J. Liang, Z. Zhao, A. Liu and Y. Tian, *Talanta*, 169 (2017) 37.
  37. Y. Li, H. Wang, B. Yan and H. Zhang, *J. Electroanal. Chem.*, 805 (2017) 39.
  38. Z. Yan, B. Fu, J. Chen, T. Liu and K. Li, *Int. J. Electrochem. Sci.*, 13 (2018) 1556.
  39. F. Ye, C. Feng, J. Jiang and S. Han, *Electrochim. Acta*, 182 (2015) 935.
  40. N.B. Messaoud, M.E. Ghica, C. Dridi, M.B. Ali and C.M.A. Brett, *Sensor Actuat. B-Chem.*, 253 (2017) 513.

© 2019 The Authors. Published by ESG ([www.electrochemsci.org](http://www.electrochemsci.org)). This article is an open access article distributed under the terms and conditions of the Creative Commons Attribution license (<http://creativecommons.org/licenses/by/4.0/>).